Measurement of damage growth in ultrasonic spot welded joint

Smeets, E.T.B.; Rans, C.D.; Alderliesten, R.C.; Castro, Saullo G.P.; Villegas, I.F.

Publication date
2022

Document Version
Final published version

Published in
Proceedings of the 20th European Conference on Composite Materials: Composites Meet Sustainability

Citation (APA)
Smeets, E. T. B., Rans, C. D., Alderliesten, R. C., Castro, S. G. P., & Villegas, I. F. (2022). Measurement of damage growth in ultrasonic spot welded joint. In A. P. Vassilopoulos , & V. Michaud (Eds.), *Proceedings of the 20th European Conference on Composite Materials: Composites Meet Sustainability: Vol 3 – Characterization* (pp. 439-447). EPFL Lausanne, Composite Construction Laboratory.

Important note
To cite this publication, please use the final published version (if applicable).
Please check the document version above.

ECCM 20

26-30 JUNE 2022

LAUSANNE SWITZERLAND

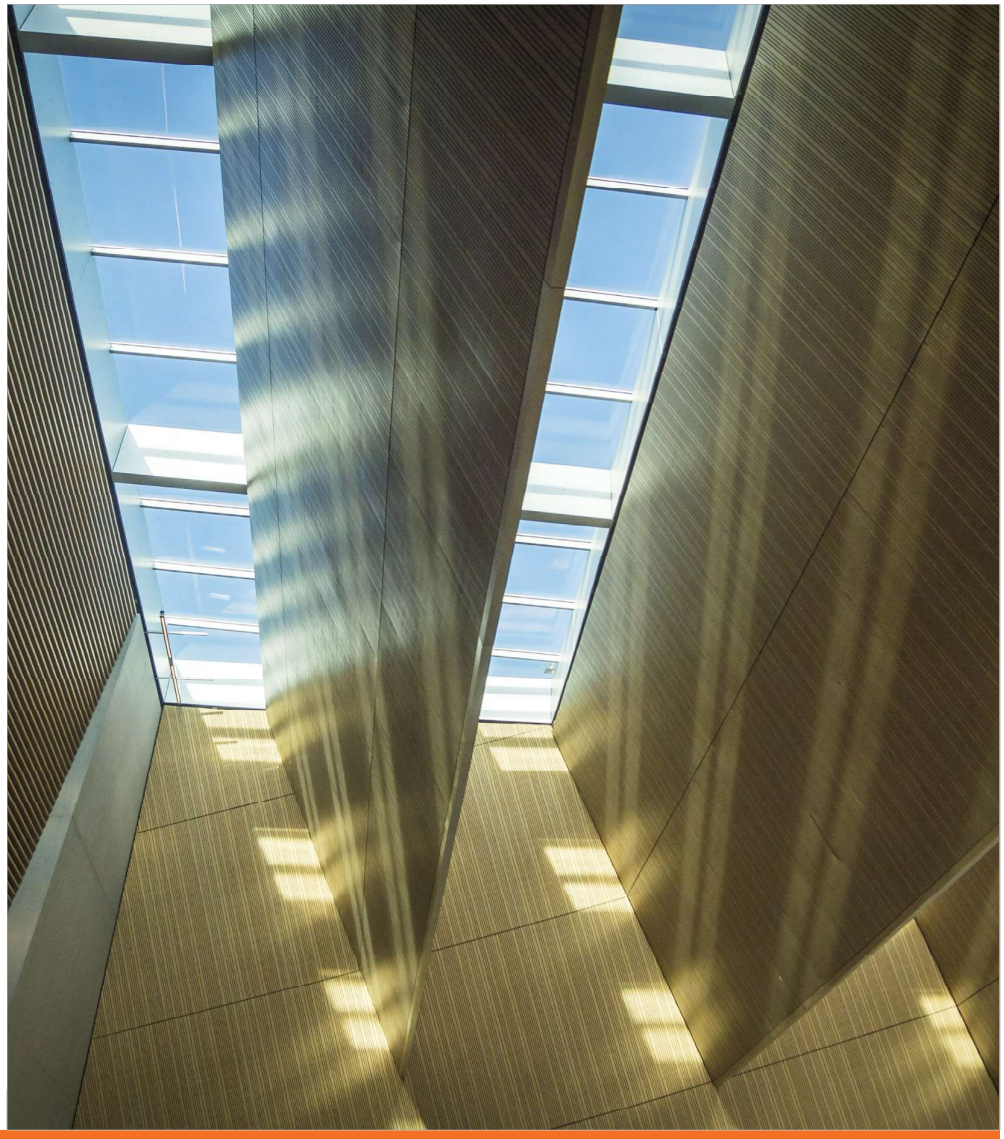

Proceedings of the 20th European Conference on Composite Materials

COMPOSITES MEET SUSTAINABILITY

Vol 3 – Characterization

Editors : Anastasios P. Vassilopoulos, Véronique Michaud

Organized by :

EPFL

Under the patronage of :

CCLAB Composite Construction Laboratory

LPAC Laboratory for Processing of Advanced Composites

ESCM EUROPEAN SOCIETY FOR COMPOSITE MATERIALS

ECCM 20
26-30 JUNE 2022
LAUSANNE SWITZERLAND

EPFL CCLAB Composite Construction Laboratory LPAC Laboratory for Processing of Advanced Composites

Proceedings of the 20th European Conference on Composite Materials ECCM20 26-30 June 2022, EPFL Lausanne Switzerland

Edited By :

Prof. Anastasios P. Vassilopoulos, CCLab/EPFL
Prof. Véronique Michaud, LPAC/EPFL

Oragnized by:

Composite Construction Laboratory (CCLab)
Laboratory for Processing of Advanced Composites (LPAC)
Ecole Polytechnique Fédérale de Lausanne (EPFL)

ISBN: 978-2-9701614-0-0
DOI: http://dx.doi.org/10.5075/epfl-298799_978-2-9701614-0-0

Published by :

Composite Construction Laboratory (CCLab)
Ecole Polytechnique Fédérale de Lausanne (EPFL)
BP 2225 (Bâtiment BP), Station 16
1015, Lausanne, Switzerland

https://cclab.epfl.ch

Laboratory for Processing of Advanced Composites (LPAC)
Ecole Polytechnique Fédérale de Lausanne (EPFL)
MXG 139 (Bâtiment MXG), Station 12
1015, Lausanne, Switzerland

https://lpac.epfl.ch

Cover:

Swiss Tech Convention Center
© Edouard Venceslau - CompuWeb SA

Cover Design:

Composite Construction Laboratory (CCLab)
Ecole Polytechnique Fédérale de Lausanne (EPFL)
Lausanne, Switzerland

©2022 ECCM20/The publishers

Disclaimer:

MEASUREMENT OF DAMAGE GROWTH IN ULTRASONIC SPOT WELDED JOINTS

Eva Smeets[a], Calvin Rans[a], René Alderliesten[a], Saullo Castro[b], Irene F. Villegas[b]*

a: Structural Integrity & Composites Group, Aerospace Structural & Materials, Delft University of Technology, Delft, the Netherlands
b: Aerospace Structures & Computational Mechanics Group, Aerospace Structural & Materials, Delft University of Technology, Delft, the Netherlands
* Corresponding author's email: e.t.b.smeets@tudelft.nl

Abstract: *Ultrasonic spot welding is a joining technique for thermoplastic composites with great potential regarding processing speed and cost. To investigate the damage tolerance and possible inherent damage arresting behavior of multi-spot welded joints, a technique is necessary to measure damage growth in the joints under cyclic loading. Visual inspection is not possible because the damage is not located on the outside surface and conventional techniques such as C-scan are not practical during a fatigue test because the specimen would have to be removed from the setup. This paper details a methodology for quantifying damage growth rates in single-spot welded joints using surface strain measurements made by Digital Image Correlation. This represents the first step towards developing a methodology for quantifying damage progression behavior in complex multi-spot welded joints.*

Keywords: damage growth; ultrasonic spot welding; thermoplastic composites; Digital Image Correlation (DIC), fatigue

1 Introduction

Thermoplastic composites present the opportunity to use fusion bonding, or welding, as a joining technique instead of mechanical fastening or adhesive bonding. Fusion bonding is particularly interesting to the aerospace industry since it is fast and cost-effective [1, 2], and eliminates many surface preparation and process control needs related to adhesive bonding [3]. The specific fusion bonding technique of ultrasonic welding provides an additional opportunity for structural joints with the possibility to tailor the damage tolerance and progressive failure behavior. The damage in these ultrasonically welded joints is confined to the welded region rather than growing through the adherends [4]. This means that the individual weld locations in a spot welded joint contain the growth of discrete damage sources, and the progression of damage to adjacent welds requires a new damage initiation event. To investigate and exploit this possibility, however, a robust methodology for quantifying the damage progression behavior in these joints is required.

Monitoring damage progression in an ultrasonically spot welded joint is hampered by the very feature of damage growth that we would like to exploit – damage growth is contained between the adherends. The study in this paper is limited to circular spot welds at the center of the specimen, which are not visible from the outside. Thus, direct observations of the damage growth are not possible. Non-destructive testing techniques such as C-scan can provide information about damage shape and size, however, this technique becomes less practical for continuous monitoring of damage progression during a fatigue test due to the

  doi:10.5075/epfl-298799_978-2-9701614-0-0

need to remove the specimen from the testing machine for inspection. This paper investigates an alternative indirect approach to monitoring the damage progression behavior using surface strains measured with the Digital Image Correlation technique (DIC). This technique has quickly become a staple measurement technique in laboratories for strain measurement but has also been successfully used in past studies for monitoring hidden interface damages. This paper will specifically look at the advantages and challenges of applying it on ultrasonically spot-welded joints.

2 Methodology

This study aims to investigate the suitability of using DIC as a quantitative method for indirectly monitoring damage progression behavior in ultrasonically spot-welded joints. To carry this out, displacement-controlled fatigue tests of single lap shear joints with a single spot weld (similar to previous studies by Choudhary and Villegas [5]) are conducted. The dimensions of the test specimens are shown in

Figure 1, the loading is applied in the horizontal direction. The lay-up of the adherends is $[0/135/90/135/45/135]_s$ and the ply material is carbon fiber with LMPAEK resin. Fatigue testing is conducted using a displacement associated with 80% of the B-basis static strength of 10 single-spot welded specimens, with a loading ratio of 0.2 and testing frequency of 5 Hz. As the focus of this paper is to examine the damage monitoring potential of DIC, the remainder of the methodology section focusses on describing the measurement and data processing methods used in the study.

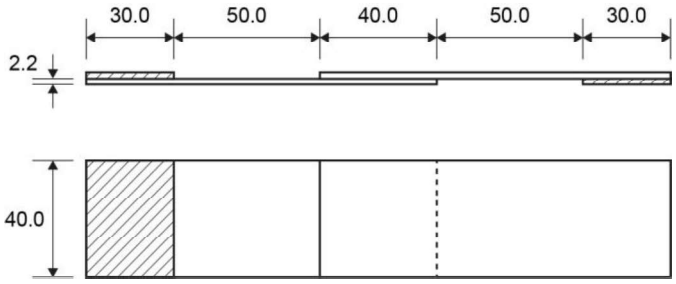

Figure 1. Dimensions in [mm] of the single lap shear specimens.

2.1 Experimental measurements

During the fatigue tests, the reaction force in the specimens is recorded by the testing machine with a peak-valley detection so that the maximum and minimum force in each cycle is registered. At every 50th cycle, a two second dwell at the maximum displacement is programmed to facilitate image capturing with two stereoscopic camera pairs for DIC measurements. The two pairs of cameras each consisting of two Grasshopper 3 (model: GS3-U3-23S6C-C) cameras are used to monitor the front and back side of the specimen. The cameras at the front of the specimen have a 50 mm lens and the ones at the back have a 28 mm lens. However, the cameras on both sides are positioned such that they have a similar field of view that maximizes the overlap region of the specimen.

  doi:10.5075/epfl-298799_978-2-9701614-0-0

2.2 Data processing

The DIC images are first processed with the Vic-3D 8 software [6] to correlate the stereo images and obtain the local displacement in all three directions. From this displacement field, a virtual extensometer can be defined to track the global compliance change of the specimen and the displacement field is converted to a strain field using a Lagrangian finite strain formulation.

Once the strains in the two principal directions (ε_{xx} and ε_{yy}) are obtained, the data is smoothed using Arbocz [7] half-wave cosine function, which can be written as:

$$f = \sum_{j=0}^{n} \sum_{i=0}^{m} cos\left(\frac{i\pi x}{L}\right)\left(A_{ij}\, cos(j\theta) + B_{ij}\, sin(j\theta)\right) \quad (1)$$

where A_{ij} and B_{ij} are the amplitudes of the corresponding shape functions. The first partial derivative $\partial f/\partial y$ is:

$$\frac{\partial f}{\partial y} = \sum_{j=0}^{n} \sum_{i=0}^{m} cos\left(\frac{i\pi x}{L}\right)\, j\,\left(-A_{ij}\, sin(j\theta) + B_{ij}\, cos(j\theta)\right) \quad (2)$$

The coefficients A_{ij} and B_{ij} are calculated based on measured data using for example a linear least-squares algorithm. In theory, m and n can be chosen for any desired accuracy, but in practice the least-squares algorithms require a high amount of computer memory that limits the maximum values for m and n. In the present work, the diccp Python module version 0.1.7 [8, 9] is used to determine the A_{ij} and B_{ij} coefficients.

Once the noise is filtered from the experimental data by excluding the high frequency terms from the half-wave cosine formulation, a five step process is followed:

1. Choose 5 vertical probing lines along the surface of the overlap (Figure 2 a and b). The data is transformed such that both sides of the specimen use the same coordinate system. The choice to use 5 probing lines was made to provide enough detailed information while not using too much computational power during the processing of the data.
2. Extract the data along the probing lines (Figure 2c).
3. Find local minima and maxima on the 5 probing lines on both sides of the specimen using the partial derivative $\partial f/\partial y$ (Figure 2c). The data from both sides is combined to get a complete view of the damage state. On the front side the data from the top half of the overlap is used and on the back side the data from the bottom half is used.
4. Figure 2d shows that the false positives are located outside of the weld boundary and at the centerline of the weld. These false positives are removed from the calculations. This is done by first identifying which points are located within the initial boundary of the weld and afterwards removing the points that are not the outer two points on each probing line, thus removing the false positives around the centerline.
5. Determine weld area by summing the areas of the 5 probing lines as shown in Figure 3. The damage is represented as a percentage of the initial weld area.

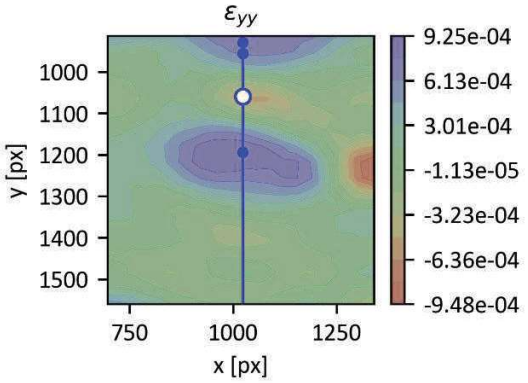

a. *Surface plot with a single probing line and extracted points on the front of the specimen.*

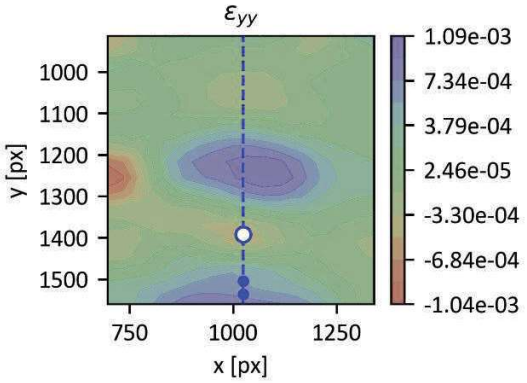

b. Surface plot with a single probing line and extracted points on the back of the specimen.

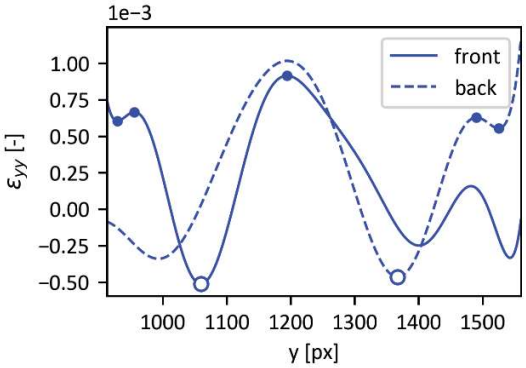

c. Line plots of the center probing lines on the front and the back of the specimen.

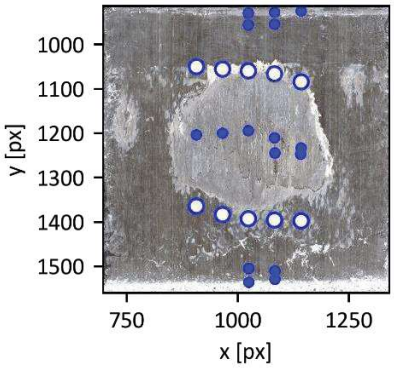

d. Fracture surface with the locations of the extracted points

Figure 2. Processing the DIC data. Points on the weld edge are indicated with open dots ○, false positives with closed dots ●.

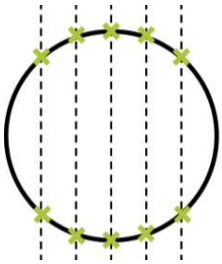

a. Estimated weld height based on each probing line.

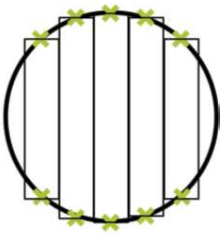

b. Estimated weld area based on each probing line.

Figure 3. Weld area estimation based on extracted weld edges.

These steps are performed for each DIC data point so that the damage progression through the fatigue life can be plotted. The data is then smoothed with the incremental polynomial method from the ASTM standard E647 [10] to calculate the damage growth rate.

3 Results

Figure 4 shows the fracture surface for two of the test specimens. The weld location is determined using the previously described methodology for four different moments during the fatigue life of the specimens.

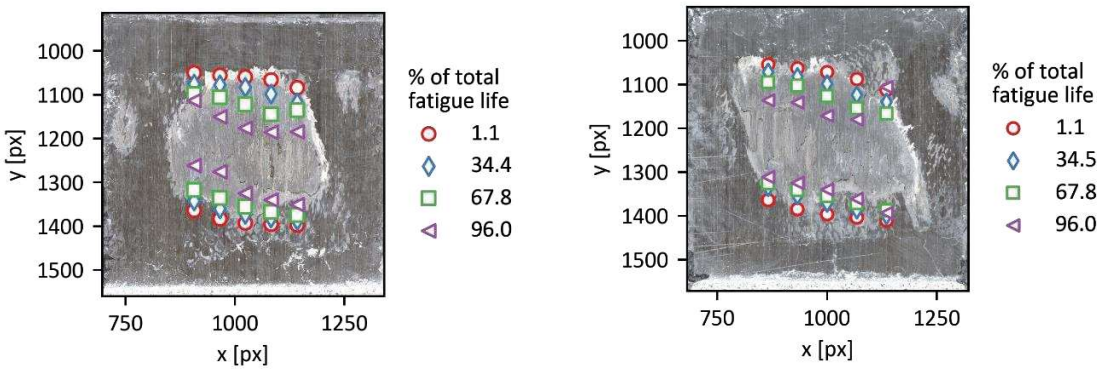

a. Extraction for test specimen 1. *b. Extraction for test specimen 2.*

Figure 4. Extracted weld edges for two different specimens at four moments during the fatigue life.

The damage evolution through the whole fatigue life is determined by performing the post-processing steps for every DIC measurement point. The result for the same two specimens can be seen in Figure 5. The smoothed result of the incremental polynomial method from the ASTM standard E647 [10] is also included.

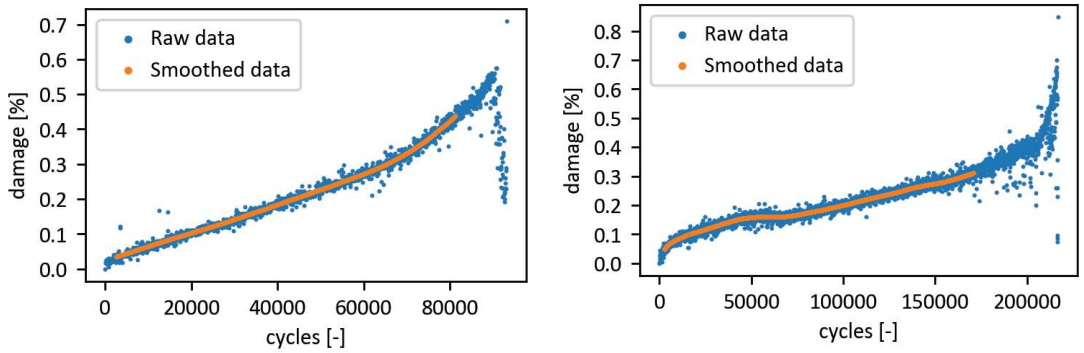

a. Damage evolution for test specimen 1. *b. Damage evolution for test specimen 2.*

Figure 5. Damage evolution through the fatigue life for two different test specimens.

4 Discussion

The raw strain data obtained from the DIC is fitted with a half-cosine Fourier fitting to filter the noise and obtain continuous functions. Figure 6 shows the strain in vertical direction over the center of the overlap fitted with two different numbers of coefficients. An increasing number of coefficients leads to the inclusion of higher frequency components. Therefore, the fitted function approaches the raw data with more accuracy, but more noise is included as well. A total of 6 coefficients was chosen to proceed with the analysis.

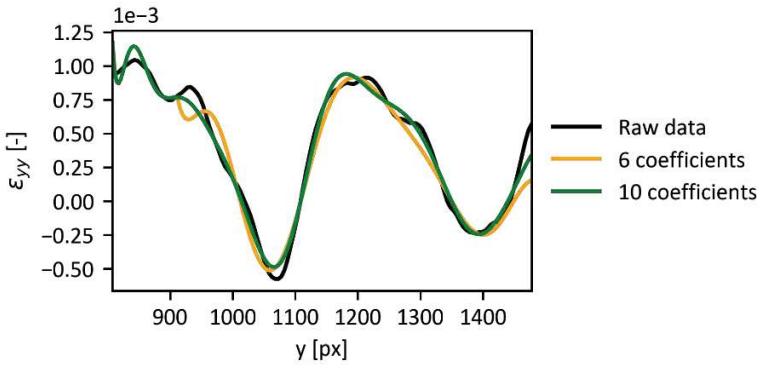

Figure 6. Half-cosine Fourier fitting of the raw DIC data with different numbers of coefficients

The information from the DIC measurements on both sides of the specimens is combined to get a full view of the overlap area, relying on the assumption that the growth of damage occurs from both sides of the centerline and does not cross the centerline of the overlap from either side. This assumption only has a small effect on the estimated damage percentage in single spot joints if there are no secondary welds. After the measurements are combined, the false positives are filtered from the extracted points by finding the two most outer points on each probing line within the weld area.

The comparison of the extracted points and the fracture surface in Figure 4 shows that the actual physical weld size is overestimated, which is especially visible when comparing the extraction at the start of the fatigue life to the complete fracture surface. When comparing the extraction at the end of the fatigue life, this comparison shows that large damages are difficult to extract, herein attributed to the fact that secondary bending is dominant when the damage has grown to most of the initial weld area.

Figure 5 shows the extracted weld area of two different specimens through their whole fatigue life. Since this data is oversampled, it is smoothed using the incremental polynomial technique as described in the ASTM standard E647 [10]. Figure 7 shows the comparison of the damage percentage after the smoothing and the compliance during the fatigue life and Figure 8**Error! Reference source not found.** shows the damage growth rate and the change in compliance. Both graphs show a good comparison between the global compliance in the specimen and the damage in the weld.

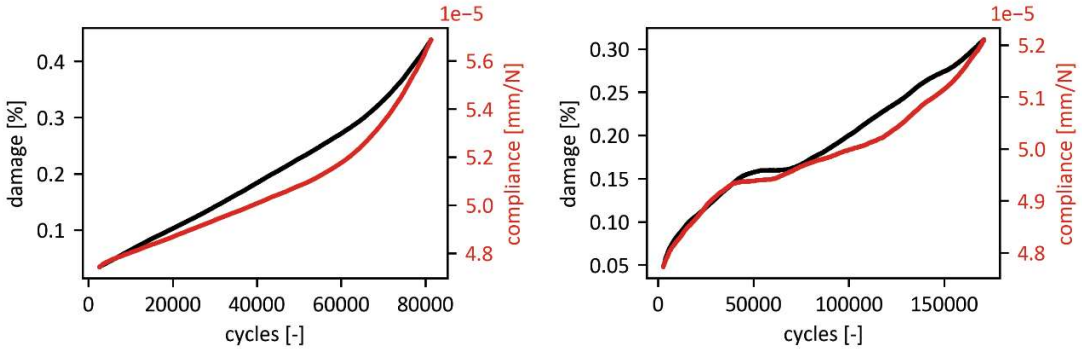

a. Damage evolution for test specimen 1 *b. Damage evolution for test specimen 2*

Figure 7. Damage evolution and compliance for the two same specimens during the fatigue life.

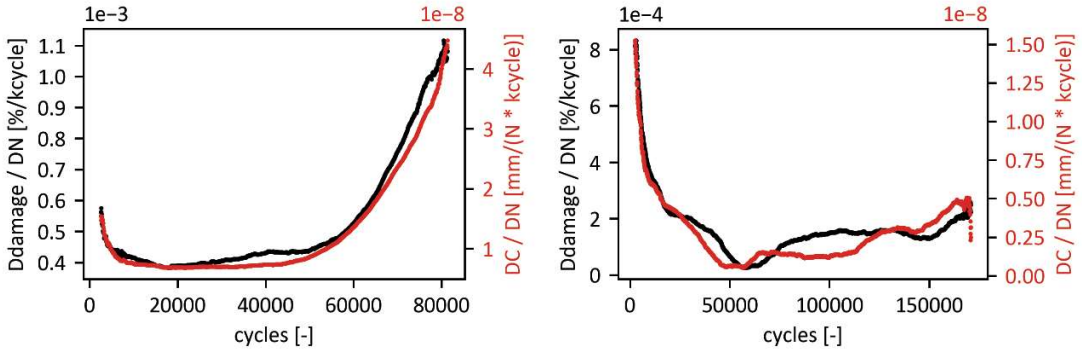

a. Damage growth rate for test specimen 1 *b. Damage growth rate for test specimen 2*

Figure 8. Damage growth rate and change of compliance versus number of cycles.

While the overall evolution of the damage is well captured, small deviations can be observed in the comparison with the global compliance (in Figure 7), specifically in the middle of the fatigue life. These differences can be attributed to damage growth in the horizontal direction. Note that the proposed method only captures growth in the direction of the loading, since the features in the other direction are too small to be captured.

Some remarks can be made regarding the expansion of this method to the analysis of multi-spot joints. First, the assumption in the combination of the measurement data, that the damage only grows on either side of the centerline, does not always hold. For example, if several spots are aligned in the direction of loading, the damage might only grow on one side of the overlap and the spots are not located in the center of the specimens. Second, in this method two points are chosen on every probing line, making it difficult to know when a weld is fully damaged. In the current test, this is not crucial information because the joints only consist of a single weld, therefore joint failure and spot failure are identical. However, in the case of multi-spot specimens, this is much more relevant information, for instance to be able to determine the sequence of failure since the failure of a single spot in the configuration does not immediately mean that the complete joint also failed. Both considerations must be addressed in the future testing campaign, when a series of multi-spot specimens with different configurations will be tested in experiments that are similar to those described in the present paper.

  doi:10.5075/epfl-298799_978-2-9701614-0-0

5 Conclusion

This paper discussed the characterization of damage growth in ultrasonically spot welded joints with use of surface strain measured by a Digital Image Correlation (DIC) system. The raw DIC data was first filtered with a half-cosine Fourier function with six coefficients. The resulting continuous functions were used to locate the local minima and maxima of the strain in vertical direction. After filtering out false positives, a view of the damage state was obtained.

After the test was completed, the fracture surface could be observed and compared to the extracted points at different moments, showing that the exact physical weld area cannot be captured with great accuracy.

When the extraction procedure was performed on every measurement point, a damage growth curve was obtained. The comparison of the damage percentage and the specimen compliance as well as the change in damage and change in compliance over the course of the fatigue life showed that a good representation of the damage evolution was obtained. Small deviations could be observed between the damage and compliance results, which were attributed to a growth of the damage in the horizontal direction, that was not captured with the current method.

It is concluded that the proposed method does allow to measure and observe the evolution of the damage growth in an ultrasonically spot welded joint. However, one should always keep in mind that the proposed damage detection methodology consists of an indirect measurement that still requires further validation against direct damage detection methods such as C-scan measurements.

6 References

1. Villegas IF, Moser L, Yousefpour A, Mitschang P, Bersee HEN. Process and performance evaluation of ultrasonic, induction and resistance welding of advanced thermoplastic composites. Journal of Thermoplastic Composite Materials. 2012;26(8):1007-24.
2. Grewell D, Benatar A. Welding of plastics: Fundamentals and new developments. International Polymer Processing. 2007;22(1):43-60.
3. Villegas IF, Bersee HEN. Ultrasonic welding of advanced thermoplastic composites: An investigation on energy-directing surfaces. Advances in Polymer Technology. 2010;29(2):112-21.
4. Zhao T, Palardy G, Villegas IF, Rans C, Martinez M, Benedictus R. Mechanical behaviour of thermoplastic composites spot-welded and mechanically fastened joints: A preliminary comparison. Composites Part B: Engineering. 2017;112:224-34.
5. Choudhary A, Fernandez I. Robotic sequential ultrasonic welding of thermoplastic composites: process development and testing. American Society for Composites 2021: Destech Publications, Inc.; 2021.
6. Correlated Solutions. Vic-3D 8. Available from: https://correlatedsolutions.eu/software/vic-software/.
7. Arbocz J. The imperfection data bank, a mean to obtain realistic buckling loads. Journal of Applied Mechanics. 1982:535-67.
8. Castro SGP. Digital Image Correlation Post Processing module Version 0.1.7. Available from: https://pypi.org/project/dicpp/0.1.7/.

  doi:10.5075/epfl-298799_978-2-9701614-0-0

9. Castro SGP, Almeida Jr JHS, St-Pierre L, Wang Z. Measuring geometric imperfections of variable–angle filament–wound cylinders with a simple digital image correlation setup. Composite Structures. 2021;276:114497.
10. ASTM Standard E647, 2016, "Standard Test Method for Measurement of Fatigue Crack Growth Rates", ASTM International, West Conshohocken, PA, 1978, DOI:10.1520/E0647-15E01, www.astm.org

